INTERNATIONAL JOURNAL OF ELECTRONICS, MECHANICAL AND MECHATRONICS ENGINEERING
Vol.9 Num.3 - 2019 (1705-1718)

IJEMME

Received: 11.05.2019
Accepted: 15.06.2019

Synthetic Aperture Radar Signal Processing

Abubakar YAOUBA[1], Necip Gökhan KASAPOĞLU[2]

Abstract *- Synthetic aperture radar signal processing is a two-dimensional operation consisting of the range compression and the azimuth compression. SAR signal processing is very important for generating and processing of various data products for different applications and analysis of the target features. The SAR raw data are 2D array of sampled echoes in complex form. The practicality of the algorithms for SAR signal processing are used to compress the energy of the echoes, thereby increasing the resolution of the SAR image. In this work, it is shown how the Range-Doppler and Stolt Interpolation techniques are carried out. The implementation of the differential azimuth compression (DAC) for the Stolt Interpolation algorithm is presented and analyzed. The Range-Doppler and Stolt Interpolation algorithms are demonstrated in Matlab and compared.*

Keywords: ***Range-Doppler algorithm, Stolt Interpolation algorithm, differential azimuth compression, Range Cell Migration Correction, matched filter, Pulse Compression technique***

1.0 Introduction

Synthetic Aperture Radar (SAR) is a type of remote sensing technology where the radar uses the motion of a small real radar antenna mounted on a moving platform such as airplanes, satellites, high altitude balloons, UAVs or drones to synthetically produce a high-resolution 2D or 3D images of objects such as landscapes. It generates and transmits a series of coded pulses at a regular interval as the platform moves along its path. The total distance the SAR device covers at a time when the radar pulses return to the antenna creates a large synthetic antenna aperture. That is, a large virtual antenna is synthesized using the displacement of the real antenna along the track. SAR operates in the microwave band, and it interacts with the target and then collects the corresponding echoes followed by imaging. SAR remote sensing is an active remote sensing technique that provides a fine spatial resolution 2D data. Fine resolution is independent of the altitude of the sensor, so images with the same geometric resolution can be obtained from the satellite as from airplanes. SAR's day-and-night imaging capability, weather independence, penetration of radar wave, geometric resolution and independence of distance, makes it one of the most popular imaging system for remote sensing.

[1] *https://orcid.org/0000-0002-8437-8064*
[2] *Department of Electrical and Electronics Engineering, Istanbul Aydin University, Istanbul, Turkey, gokhankasapoglu@aydin.edu.tr, https://orcid.org/0000-0001-9649-4751*

2.0 Radar modulation techniques

Radars are able to determine the distance of an object from their sensors. They are also capable to determine the speed of a moving object. This can be done by timing the delay from when the chirp signal is transmitted and to when the echo signal is received, or by determining the frequency difference between the transmitted chirp signal and the echo signal. The timing of the pulse delay employs the AM technique while the detection of the frequency difference and ranging employ the linear FM technique.

2.1 Frequency modulation (FM) technique.

In Frequency modulation (FM) technique the frequency of the carrier is varied in accordance with some characteristic of the baseband modulating signal $\mathrm{S_b(t)}$

$$S(t) = \mathrm{A_0 exp}\left[\mathrm{j}(\omega_c \mathrm{t} + \alpha \int_{-\infty}^{\mathrm{t}} \mathrm{S_b(t)dt})\right]$$

Since baseband-modulating signal $S_b(t)$, is normally a sinusoidal function, then

$$S(t) = \mathrm{A_0 exp}\left[\mathrm{j}(\omega_c \mathrm{t} + \alpha \int_{-\infty}^{\mathrm{t}} \cos(2\pi f_a \mathrm{t})\mathrm{dt})\right] = \mathrm{A_0 exp}[\mathrm{j}(2\pi \mathrm{f_c t} + \alpha \sin\omega_a t)] \quad (1)$$

Where α is the maximum value of the phase deviation and is known as modulation index. $\mathrm{f_c}$ is the carrier frequency. By differentiating the instantaneous phase of $\mathrm{S(t)}$, we obtain the instantaneous frequency f, as

$$f = {}^{1}\!/_{2\pi} \frac{d}{dt}\left[w_c t + \alpha \int_{-\infty}^{t} S_b(t)dt\right] = f_c + \frac{1}{2\pi}\alpha \mathrm{S_b(t)} \quad (2)$$

2.2 Linear Frequency Modulation (LFM) technique.

The transmitter frequency is either continually increasing or continually decreasing from the reference frequency. The transmitted FM is modified in order to be linear with time.

From the instantaneous frequency obtained in equation 2.

$$f = f_c + \frac{1}{2\pi}\alpha \mathrm{S_b(t)} = f_c + k_r t,$$

Where $\alpha \mathrm{S_b(t)} = 2\pi k_r t$ and k_r is known as the chirp rate (frequency changing rate) and is given as,

$$k_r = {}^{\mathrm{df}}\!/_{\mathrm{dt}}$$

Therefore $\mathrm{S(t)} = \mathrm{A_0 exp}\left[\mathrm{j}(\omega_c \mathrm{t} + \alpha \int_{-\infty}^{\mathrm{t}} \mathrm{S_b(t)dt})\right] = \mathrm{A_0 exp}\left[\mathrm{j}(\omega_c \mathrm{t} + \int_{-\infty}^{\mathrm{t}} 2\pi k_r t dt\right]$

$$\mathrm{S(t)} = \mathrm{A_0 exp}(\mathrm{j}2\pi \mathrm{f_c t} + \mathrm{j}\pi k_r t^2) \quad (3)$$

There are two common forms of LFM used in radar application: the chirp or the Pulsed LFM and the continuous-wave LFM.

2.3 The Pulsed Linear Frequency Modulation (PLFM) Radar

Lets $p_1(t)$ be defined as

$$p_1(t) = Rec\left(\frac{t-{}^{\tau_p}/_2}{\tau_p}\right)$$

Where the rectangular rect(t) is defined as

$$\text{rect(t)} = \begin{cases} 1, & |t| \le \frac{1}{2} \\ 0, & |t| > \frac{1}{2} \end{cases},$$

and let $p_2(t) = \mathrm{A_0 exp[j(2\pi f_c t + \pi k_r t^2)]}$

The Pulsed symmetrical LFM signal S(t) with pulse duration τ_p is gotten as follows;

$$\mathrm{S(t)} = p_1(t).p_2\left(t - {}^{\tau_p}/_2\right)$$

$$= Rec\left(\frac{t-{}^{\tau_p}/_2}{\tau_p}\right).\mathrm{A_0 exp}\left(\mathrm{j2\pi f_c}\left(t - {}^{\tau_p}/_2\right) + \mathrm{j\pi}k_r\left(t - {}^{\tau_p}/_2\right)^2\right) \quad (4)$$

and the Pulsed nonsymmetrical LFM signal S(t) with pulse duration τ_p as;

$$\mathrm{S(t)} = p_1(t).p_2(t) = Rec\left(\frac{t-{}^{\tau_p}/_2}{\tau_p}\right).\mathrm{A_0 exp(j2\pi f_c t + j\pi}k_r t^2) \quad (5)$$

The figures below show the time–frequency relation of a pulsed LFM

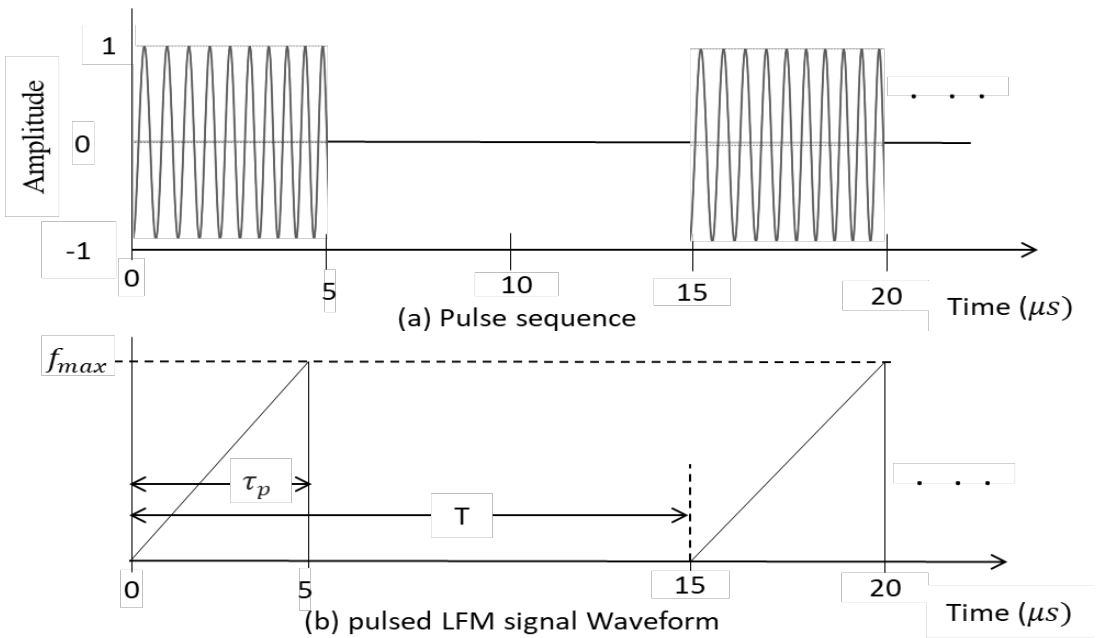

Figure 1. Lear FM pulsed train

The pulsed LFM waveform has pulse duration time τ_p where $f_{max} = k_r\tau_p$ and the frequency bandwidth is

$$B = f_{max} = k_r\tau_p \quad (6)$$

2.4 Quadrature Demodulator

Considering the LFM signal $S(t) = A_0 exp(j2\pi f_c t + j\pi k t^2)$

The real value of the signal is represented as

$$S(t) = A_0 \cos(2\pi f_c t + \pi k t^2) = A_0 \cos(2\pi f_c t + \emptyset(t)) \quad (8)$$

Where $\emptyset(t) = \pi k t^2$ is the phase term presented for illustration purposes. The carrier frequency f_c generally has a higher value as compared to kt. The time varying-phase $\emptyset(t)$ information is transmitted using the complex-valued signal. After transmitting the time-varying phase $\emptyset(t)$, information, the Quadrature demodulator is then used to acquire the correct phase information. As illustrated on figure 2 the in-phase–quadrature-phase demodulator splits any complex-valued LFM signal $s(t)$, into the real or in-phase (I), and imaginary or quadrature-phase Q, components of $\emptyset(t)$. Two carriers $\cos(2\pi f_c t)$ and $\sin(2\pi f_c t)$ are locally generated by the system. The LPF filter out high frequency component $4\pi f_c t + \emptyset(t)$ and retain the low-frequency component $\emptyset(t)$. The A/D converter digitizes the real and imaginary parts of the low frequency phase signal $\emptyset(t)$ to obtain a complex number pair that serves as a row element of the two dimensional image the radar data.

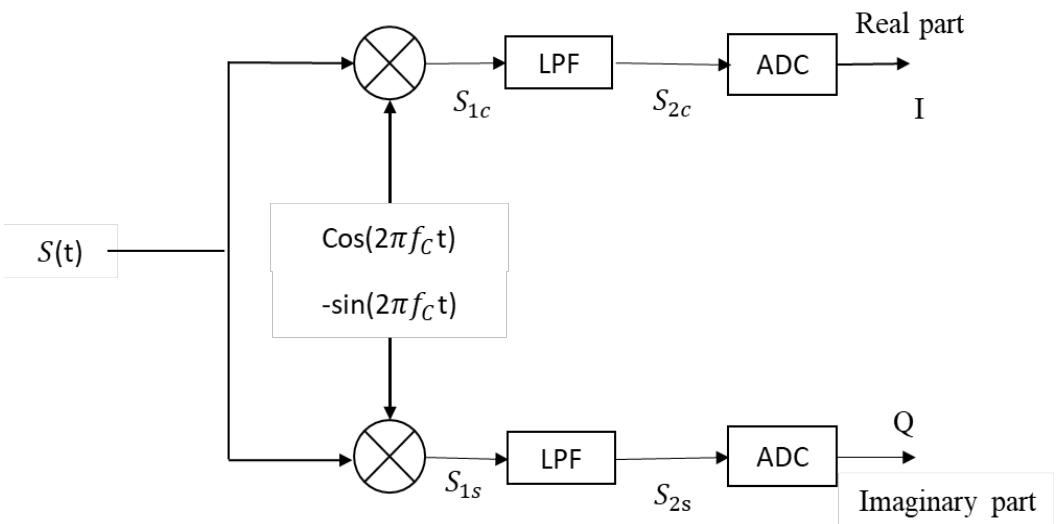

Figure 2 Quadrature demodulator

The following intermediate signals S_{1s}, S_{1c}, S_{2s} and S_{2c} are obtained as follows:

$$S_{1c}(t) = {}^1/_2 (\cos(4\pi f_c t + \emptyset(t)) + \cos(\emptyset(t))),$$

$$S_{1s}(t) = {}^1/_2 (\sin(4\pi f_c t + \emptyset(t)) + sin\emptyset(t)),$$

$$S_{2c}(t) = {}^1/_2 \cos(\emptyset(t)),$$

$$S_{2s}(t) = {}^1/_2 \sin(\emptyset(t)).$$

The time varying signal phase $\emptyset(t)$ can then be obtained as:

$$\emptyset(t) = \tan^{-1}\left(\frac{S_{2s}(t)}{S_{2c}(t)}\right) \quad (9)$$

2.5 Matched Filter and Pulse Compression technique

Matched filtering is a technique used to regain a signal that was corrupted by additive white Gaussian noise. A matched filter is applied on received signal in order to identify a target by determining whether the filter output (compressed pulse), exceeds a specific threshold. Different targets produce pulses of different magnitudes and each magnitude depends on three factors: targets reflectivity ($\boldsymbol{\sigma}$), pulse width (τ_p) and range (R) from the radar sensor to target. The effective width of a compressed pulse is determined by the bandwidth and the pulse width τ_p of the received signal

Considering an ideal target with reflectivity 1 and zero signal attenuation between the radar sensor and target area. If the input signal is x*(t)* and the Fourier transform of the input signal is *X (f),* then the matched filter *h(t)* and the Fourier transform of the matched filter H(f) can be expressed as follows:

$$h(t) = x^*(t) \quad \text{and} \quad H(f) = X^*(f)$$

If *f(t)* is the output of the matched filter, then

$$F(f) = X(f)H(f) = |X(f)|^2$$

Therefore $f(t) = \mathcal{F}^{-1}(|X(f)|^2) = x(t) * h(t) = \int x(\tau)h(t-\tau)d\tau$

For h(t)=x^*(t) , then, $f(t) = \int x(\tau)x^*(t+\tau)d\tau$.

This is the definition of autocorrelation of x(t). That is the matched filtering of any signal x*(t)* is equivalent to the autocorrelation of that signal x*(t)* with itself. Consider the echo of a non-symmetric LFM signal *S(t)* to be the echo signal from single target:

$$S(t) = Rec\left(\frac{t-\tau_p/2}{\tau_p}\right).A_0\exp(j2\pi f_c t + j\pi k t^2)$$

If $A_0 = 1$ and *h (t)*= x*(t)*, then the output of the matched filter is given as:

$$f(t) = \int_0^{\tau_p} s(\tau)s^*(t+\tau)d\tau = \left[-j\left(2\pi f_c t + \pi k t\tau_p + \pi k t^2\right)\right].T.\text{sinc}\left(kt\tau_p\right) \qquad (10)$$

Since convolving of two signals in the time domain is same as multiplying the two signals in the frequency domain, therefore, the matched filter will be implemented by first transforming the received signal and the matched filter function into frequency domain using Fast Fourier Transform. The resulting product of the frequency domain functions are then converted back to time domain by applying Inverse Fast Fourier Transform. Matched filter function is shorter than the received signal because of different ranges of different targets. For this reason, paddings with zeros on the matched filter function is required when applying the Fast Fourier Transform on the matched filtering. Figure 3 below shows the block diagram of DFT-based pulse compression process.

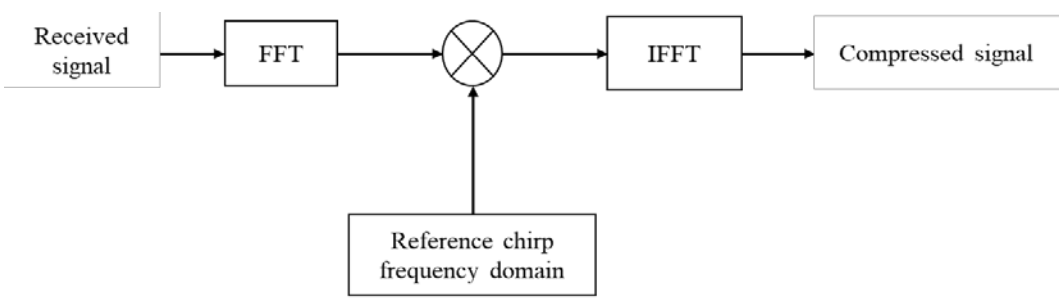

Figure 3 Block diagram of DFT-based pulse compression

3.0 SAR raw data generation

From equation 5, the PLFM radar waveform:

$$S(t) = Rec\left(\frac{t-{}^{\tau_p}/_2}{\tau_p}\right).A_0 exp(j2\pi f_c t + j\pi k_r t^2)$$

With a rectangular gate function $\left(\frac{t}{\tau_p}\right)$, pulse duration time τ_p, amplitude of transmitted signal A_0, and PLFM chirp rate k_r. The chirp signal starts and end at $t = 0$ and τ_p respectively. Let suppose the gate function is $\alpha(t)$ and the amplitude A_0 as 1. Considering the echoes are from I different reflectors, with reflective coefficient σ_i corresponding to ranges R_i, where $i = 1, 2, 3, \ldots, I$, then the signal S(t) written as the sum of delayed echoes is

$$S(t) = \sum_{i=1}^{I} \sigma_i \alpha(t - {}^{2R_i}/_c) \ .exp\left\{j2\pi f_c\left(t - {}^{2R_i}/_c\right) + j\pi k_r\left(t - {}^{2R_i}/_c\right)^2\right\}$$

$$= \sum_{\mathbf{i=1}}^{\mathbf{I}} \boldsymbol{\sigma_i \alpha(t-\tau_i)} \ .\mathbf{exp\{j2\pi f_c(t-\tau_i) + j\pi k_r(t-\tau_i)^2\}} \quad (11)$$

Where $\tau_i = {}^{2R_i}/_C$ is the echo delay time from the ithtarget. Considering that the target location at any point $(x_i,\ y_i)$ with radar the position at $(0,\ 0)$ at an altitude 0, then τ_i can be calculated as:

$$\tau_i = 2\left(\frac{\mathrm{R_i}}{\mathrm{c}}\right) = 2\left(\frac{\sqrt{\mathrm{x_i^2+y_i^2}}}{\mathrm{c}}\right) \quad \text{and the range is calculated as } \ R_i = \frac{1}{2}(c\tau_i)$$

The baseband signal $S_b(t)$ can be obtained through the quadrature demodulation process by first removing the frequency of the carrier and applying a low pass filter (LPF). The demodulated baseband signal can be obtained as:

$$S_b(t) = \sum_{i=1}^{I} \sigma_i |\alpha(t-\tau_i)|^2 \, exp\{-j2\pi f_c \tau_i + j\pi k_r (t-\tau_i)^2\}$$

If η is the time index of the demodulated signal, then the baseband signal $S_b(t)$ can be express in terms of n as:

$$\boldsymbol{S_b(t_\eta) = \sum_{i=1}^{I} \sigma_i \left|\alpha(t_\eta - \tau_i)\right|^2 \mathbf{exp}\left\{-\mathbf{j2\pi f_c \tau_i} + \mathbf{j\pi} k_r\left(t_\eta - \tau_i\right)^2\right\}} \quad (12)$$

with η = 0,1,2, . . ., Ɲ−1. Where Ɲ is the total number of range samples receive. Ɲ is a function pulse duration time, number of targets, and sampling frequency. The signal in 12. is based on a single pulse duration transmitted from a single position. Suppose the radar is moving along the azimuth direction (direction perpendicular to the radar beam) emitting signal at pulse repetition frequency f_{PRF}, then a two dimensional received data array will be obtain.

Suppose the moving radar position along the azimuth is u_m, where $m = 1,\ 2,\ 3, \ldots, \mathrm{M}$. with M as the total number of processed azimuth lines and must be greater than or equal to the number of azimuth lines (N_{az}) within the length L_s (synthetic aperture).

Therefore, 12. written in 2D is:

$$\boldsymbol{S_b(u_m, t_\eta) = \sum_{i=0}^{I} \sigma_i \left|\alpha(t_\eta - \tau_{u_m i})\right|^2 exp\left\{-j2\pi f_c \tau_{u_m i} + j\pi k_r\left(t_\eta - \tau_{u_m i}\right)^2\right\}} \quad (13)$$

Where $\tau_{u_m,i} = 2\left(\frac{R_{umi}}{c}\right)$ is the received signal delay time from the ith target with radar located at the position u_m

4.0 SAR Synthesis Algorithms

The received 2D data array synthesized from the waveform of 13 has a waveform of size M by N in both azimuth and the range (time) directions. The 2D data array is formed by M bursts of the radar pulse with N samples each. The data spread in range is caused by the time duration of the transmitted PLFM signal while the spread in azimuth is due to the fact that the target is under illumination by the radar beam during which the radar is collecting echoes in a period which the radar covers the synthetic aperture length L_s.

The main aim of processing raw data is to convert it into a single pixel in the final processing stage. There exist a number of SAR signal processing techniques. Each and every SAR signal processing technique has its advantages and disadvantages. Some of these SAR signal processing techniques which are based on matched filters include; Range-Doppler, Wave domain, Omega-K, Chirp Scaling, Spectral Analysis, Stolt interpolation. The Range-Doppler technique, the Stolt-interpolation technique and the Chirp scaling technique are implemented and discussed in this work. Each of these techniques has its own advantages in high-quality imaging or computation efficiency. For instance, the Range-Doppler technique is an accurate approximation and computationally efficient for processing radar images while Stolt interpolation technique is computationally intensive, but has advantages over the Range-Doppler technique.

4.1 Range–Doppler processing of SAR data.

There are three major tasks when processing SAR data by implemented the typical Range-Doppler processor: firstly, the range compression, followed by the cell migration correction, and lastly the azimuth compression. The range Doppler technique is displayed in figure 4

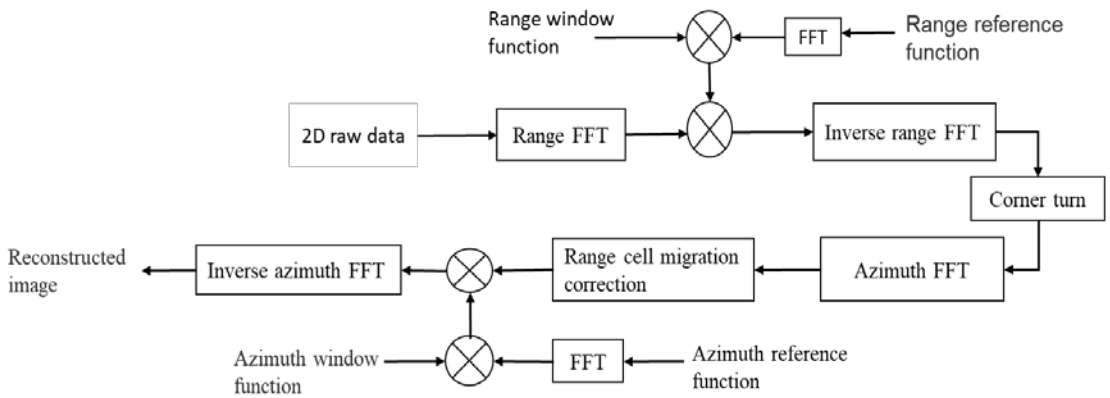

Figure 4. A flow diagram of the Range-Doppler algorithm**.**

The 2D raw data (complex data) refers to the quadrature demodulated baseband signal. The range compression is done in three steps. First by applying the range Fourier transform on the 2D complex data using the range FFT block, followed by Fourier transforming the range reference function using the FFT block and multiplying with each row of the Fourier transformed 2D complex data and lastly the is inversely Fourier Transformed using the range IFFT block. The 'corner turn' transpose the range 2D range compressed complex data from row data to column data for subsequent azimuth compression. The transposed 2D complex data is Fourier transformed to Range-Doppler domain using the azimuth FFT block. If range cell migration correction is required, then it is applied at this stage. To compress the data in azimuth, first the azimuth reference function is Fourier transformed using the FFT block and multiplied with each row of the 2D complex data in range Doppler domain and lastly followed by taking inverse azimuth FFT of the product. After azimuth compression, the resulting image is the constructed image of targets that were focused.

4.2 Stolt interpolation processing of SAR data

Figure 5. display the block diagram of Stolt interpolation processing of SAR raw data.

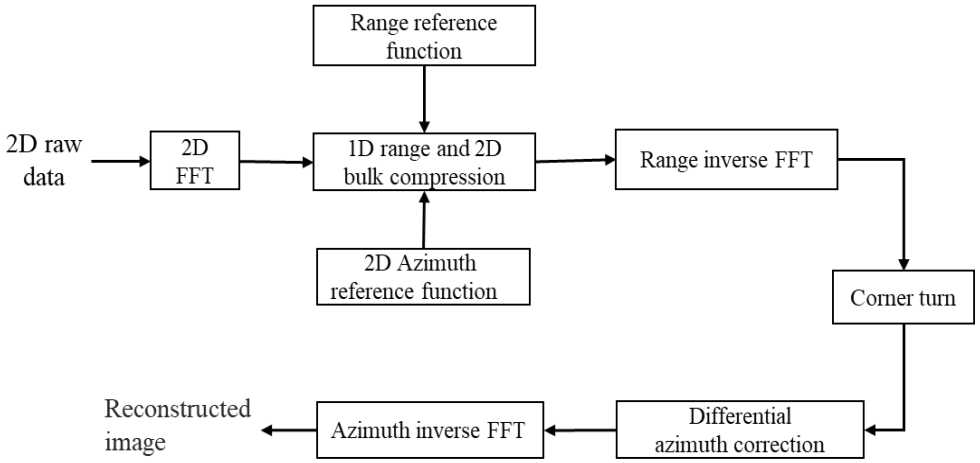

Figure 5 The diagram of Stolt interpolation algorithm processing.

4.3 Reconstruction algorithm for Stolt interpolation processing.

To compress the data in range, the 2D raw data $S_\sigma(t,u)$ is 2D Fourier transformed to $S_\sigma(\omega,\omega_{dp})$. The 2D Fourier Transformed signal $S_\sigma(\omega,\omega_{dp})$, will then be multiplied with the range matched filter $P_\sigma^*(\omega)$ to obtain a range compressed data $S_{\sigma c1}(\omega,\omega_{dp})$. The range compressed data array $S_{\sigma c1}(\omega,\omega_{dp})$ is then transformed in range–Doppler frequency domain data $S_{\sigma c1}(t,\omega_{dp})$ by taking inverse-Fourier-transformed of $S_{\sigma c1}(\omega,\omega_{dp})$.

For azimuth compression, the corresponding azimuth matched filter is obtained in following two ways:

1. By applying 1D azimuth matched filter in slow time t. With frequency changing rate k_a and the Doppler frequency f_{dp} (f_{dp}=0, for broadside case), the reference function is obtained as follows:

$$h_{af}(t) = exp(-j\pi k_a t^2),$$

where the frequency changing rate $k_a = {-2V^2}/{\lambda R_0}$ and $\Delta t = {1}/{f_{PRF}}$

The reference function $H_{af}(\omega_{Dp})$ is obtained by taking FFT on $h_{af}(t)$.

2. By applying the 2D azimuth matched filter. The 2D azimuth matched filter is obtained as follows:

$$H_{af}(\omega,\omega_{dp}) = exp\left[j\sqrt{4\left(\frac{\omega^2}{c^2}\right)-\left(\frac{\omega_{dp}^2}{V^2}\right)}X_{\mathrm{C}}\right]$$

Where ω_{dp} is the Doppler frequency in azimuth direction and ω is the time domain signal passband frequency, that is $\omega_c - \omega_0 \le \omega \le \omega_c + \omega_0$, where ω_c and $2\omega_0$ are the carrier frequency, and the bandwidth of the transmitting signal respectively. The distance X_{C} , of the radar from the center of the swath is invariant in the coordinates of the radar $(0,u)$ in stripmap SAR.

In broadside SAR, the 2D azimuth matched filter $H_{af}(\omega,\omega_{dp})$ is approximated to 1D azimuth match filter $H_{af}(\omega_{dp})$ since no range migration correction is needed while in squint SAR both the 1D and 2D reference functions are applied since it require range migration correction. Azimuth compression is carried out by multiplying each column of the range compressed data $S_{\sigma c1}(t,\omega_{dp})$ with the azimuth matched $H_{af}(\omega_{dp})$ to obtain 2D compressed data $S_{\sigma c}(t,\omega_{dp})$. After the

azimuth compression, the resulting 2D compressed signal $S_{\sigma c}(t, \omega_{dp})$ is a roughly compressed signal along azimuth direction, since only one azimuth reference function is required to perform azimuth compression on the whole data. The 2D azimuth compressed data $S_{\sigma c}(t, \omega_{dp})$ will next be processed by Stolt interpolation. Stolt interpolation improves the quality the image through differential azimuth compression based on.

$$\boldsymbol{S'_{\sigma c}(x, k_y) = S_{\sigma c}(x, k_y) exp\left[-j\left(\frac{k_y^2}{4k_c}\right)\Delta x_n\right]}$$

The differential azimuth compression requires the computation of the following terms;

First the computation of range difference $\Delta x_n = (x_n - X_c)$ where X_c and x_n are the range values along the range axis. The range difference Δx_n can be calculated as

$$\Delta x_n = {}^{c}/_{f_s}\,(n - N_r),$$

where N_r corresponds to the range sample at X_c

Second the computation of the constant phase $k_y^2/4k_c$, where $k_c = {}^{\omega_c}/_{c}$ and the azimuth value $k_y = 2\pi m f_{PRF}/VN_y$, with m = 1, 2, 3, ..., N_y.

For a given m value along the Doppler-frequency axis, the value of k_y is computed first then followed by the multiplication of every range sample $S_{\sigma c}(t, \omega_{dp})$ by $exp\left\{-j\left(\frac{k_y^2}{4k_c}\right)\Delta x_n\right\}$.

After the differential azimuth compression is applied, the final image data is obtained by taking the azimuth inverse FFT with respect to ω_{dp}.

5.0 Reconstruction of satellite radar Image using Range-Doppler processing and Stolt Interpolation algorithm.

A satellite-based (ERS) raw data generated by ESA, processed and distributed by German Aerospace Center, DLR will be used in reconstructing the radar image using Range Doppler algorithm. The parameters ERS SAR sensor parameters are listed on table 1.

	Parameters		Value	Unit
Parameters for range compression	Range sampling frequency	f_s	18.962468 x10^6	$\boldsymbol{s^{-1}}$
	Chirp rate	k_r	4.18989015x10^{11}	$\boldsymbol{s^{-2}}$
	Chirp length	τ_p	37.12x10^{-6}	s
Parameters for azimuth compression	Velocity parameter	V	7098.0194	m/s
	Wavelength	$\boldsymbol{\lambda}$	0.05656	m
	Range to target at broadside time t = 0	$\boldsymbol{R_0}$	852358.15	m
	Aperture time	$\boldsymbol{t_a}$	0.6	s
	Pulse repetition frequency	PRF	1679.902	$\boldsymbol{s^{-1}}$

Table 1. ERS sensor parameters

Figure 6 shows the ERS data. The Range Doppler technique will be applied to process the raw data.

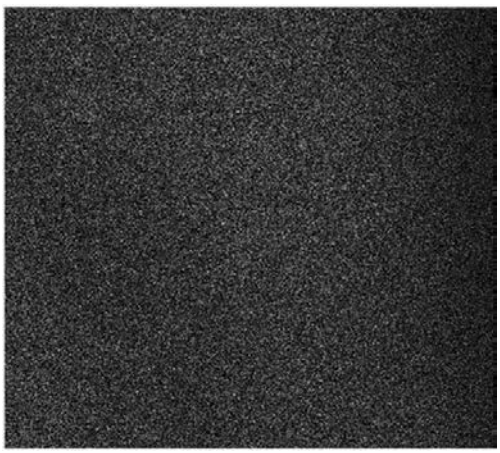

Figure 6. ERS data

The operation of range compression is performed by first transforming each row of the data into the frequency domain by applying range FFT. Since there is 704-time sample for each azimuth line, zero paddings are required for the range compression. The Fourier transformed match filter is then multiplied with every row of the frequency domain data. The range compressed data in frequency domain result is transformed back to time domain using range inverse FFT. Figure 7 shows the range compressed data.

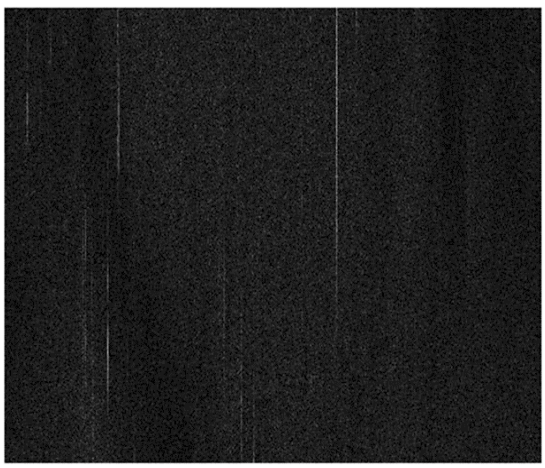

Figure 7. Range-compressed signal

To perform the azimuth compression is an azimuth reference function is applied on every column of Doppler frequency domain data. First the reference function $h_{af}(s)$ is transformed into Doppler frequency domain $H_{af}(f)$ by DFT. Since the total sample number of the azimuth reference function is 1008, zero paddings are required to increase the azimuth samples number to the total length of 2048 (length of the data). The azimuth reference function $H_{af}(f)$ is next applied on every column of the data in range-Doppler frequency domain. An inverse DFT is applied on every column of the compressed data to get the processed image. The processed image is shown on Figure 8.

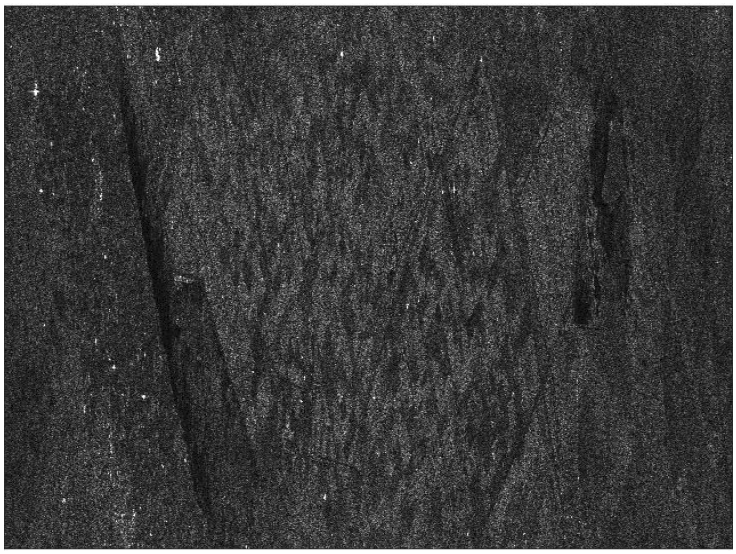

Figure 8. Constructed Image

After range compression, the next operation to perform is the azimuth compression. In azimuth compression, each column of the range compressed data and the azimuth matched filter are transformed in to Doppler frequency domain by azimuth FFT. Since The reference function $H_{af}(f)$ in Doppler frequency domain has the total number of 1008 samples, zero paddings are required to increase the azimuth samples number to the total length of 2048 (length of the data). The azimuth reference function $H_{af}(f)$ is multiplied with each column of the range-Doppler frequency domain data and the product is inversely Fourier transformed using azimuth inverse FFT to get the processed image. The processed image is shown on Figure 9.

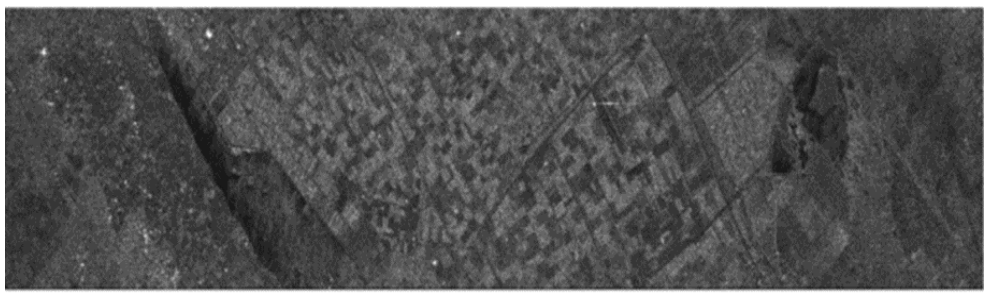

Figure 9. Image after multilook and spatial processing

To process the ERS data using Stolt interpolation, the range-compressed data array $S_{\sigma c1}(m, n')$ in figure 7 above is transformed into rang–Doppler frequency domain (t, ω_{dp}), by applying Fourier transform on each and every column of the range compressed data array $S_{\sigma c1}(m, n')$. The compressed data in the range-Doppler frequency domain (t, ω_{dp}), will then be processed by Stolt interpolation based on wavenumber domain.

Stolt interpolation starts by performing bulk azimuth compression using 1D and 2D azimuth matched filter and then applying differential azimuth compression. Since the ERS data provided is from broadside SAR, the 2D azimuth reference function is approximated to 1D reference function $H_{af}(\omega_{dp})$.

The range compressed data in range-Doppler frequency domain (t, ω_{dp}) is transformed to (ω, ω_{dp}) domain by applying FFT on each and every row of $S_{\sigma c1}(m, n)$ to get $S_{\sigma c1}(m', n)$ where $m' = 1, 2, 3, \ldots, 2048$. The 1D azimuth reference

function is then applied to $S_{\sigma c1}(m', n)$ to obtain a roughly compressed signal $S_{\sigma c2}(m, n)$ in (ω, ω_{dp}) domain. Applying a 2D inverse FFT on the bulk compressed data $S_{\sigma c2}(m, n)$, a roughly constructed image $\mathrm{I}_{\sigma}(m, n)$ with respect to $\omega, and\ \omega_{dp}$ is obtained. Figure 10 displays the roughly constructed image $\mathrm{I}_{\sigma}(m, n)$ of Stolt interpolation technique.

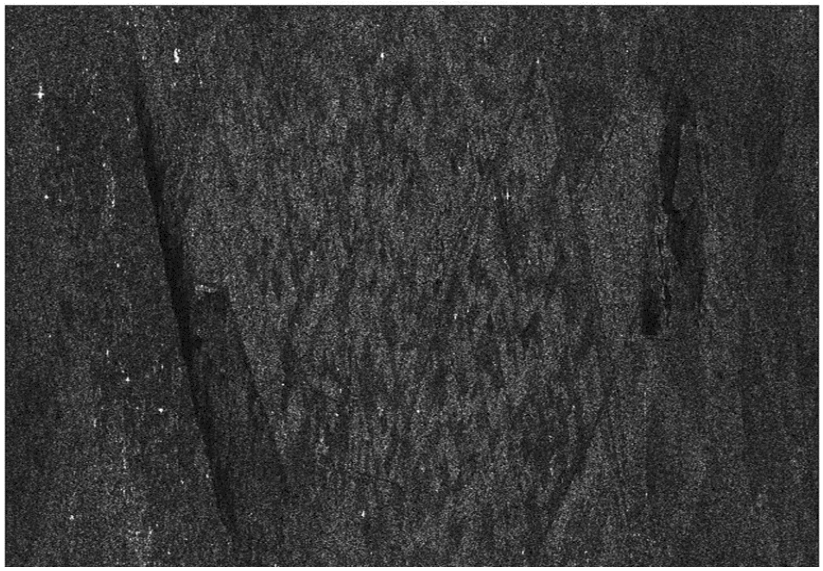

Figure 10. Processed image by Stolt interpolation technique without DAC

Comparing 10. by Stolt interpolation technique without DAC and 8 by RDA, it can be seen that the two algorithms generate images which are difficult to differentiate in terms of have quality (having similar quality). The quality of the roughly compressed image of figure 10 can further be improved by applying differential azimuth correction (DAC).

The bulk compressed data array $S_{\sigma c2}(m, n)$ in (ω, ω_{dp}) domain is inversely Fourier transformed to range Doppler frequency domain (t, ω_{dp}) before applying differential azimuth correction . To design the differential azimuth correction function, the range difference Δx_n and the phase constant k_{mc} are computed as:

$$\Delta \mathrm{x_n} = \mathrm{c}\left(\frac{\mathrm{n}-\mathrm{N_r}}{f_s}\right) \quad \text{and} \quad \mathrm{k_{mc}} = \frac{1}{4}\left(\frac{\mathrm{k_y^2}}{\mathrm{k_c}}\right)$$

Where $k_y = 2\pi m f_{PRF}/VN_y$, $\mathrm{k_c} = 2\pi f_c/c$, m = 1, 2, 3, . . ., N_y, $N_y = 2048$, n = $1, 2, 3, \ldots, N_x$, and the reference sample $\mathrm{N_r}$, equals to the range value corresponding to the slant range R_0 (or the range sample value at X_c).

The differential azimuth function is applied on the compressed data $S_{\sigma c2}(m, n)$ for the whole range samples from 1 to 2048 as in the equation form:

$$\mathrm{I_{\sigma a}}(m, n) = S_{\sigma c2}(m, n)\ \exp(-i * \mathrm{k_{mc}} * \Delta \mathrm{x_n}.)$$

After differential azimuth compression is computed on the roughly constructed image $\mathrm{I}_{\sigma}(m, n)$, then inverse Fourier Transform is applied on $\mathrm{I_{\sigma a}}(m, n)$ to obtain the final constructed image as shown in figure 11.

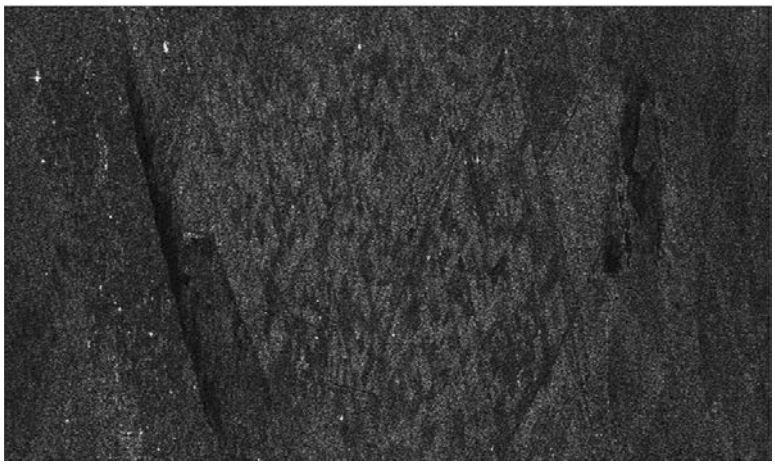

Figure 11. Processed SAR image

Applying multi-look and special filtering on the Stolt interpolation processed data, the resulting image is shown in figure 11

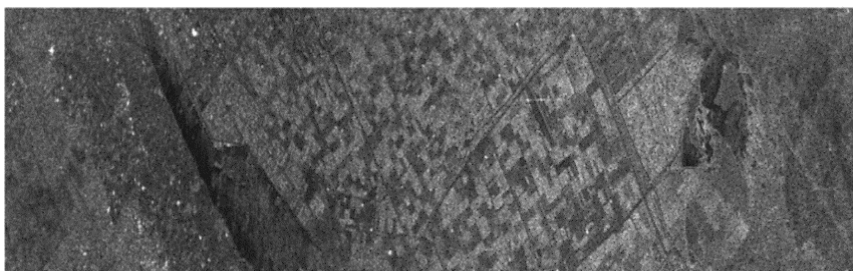

Figure 12. Image after multi-look and spatial processing

Comparing the two multi-look and spatial processed images of figure 9 and figure 12 the multi-look and spatial processing image figure 12 improves slightly in quality. This slight difference is due to the differential azimuth compression involved in the Stolt Interpolation algorithm

6.0 COMPARISON OF ALGORITHMS

The Range-Doppler algorithm is computationally efficient, flexible, less computational time and is an accurate approximation for processing of radar images but has some disadvantages with respect the high computational time to obtain good accuracy in the range cell migration correction operation. That is, it becomes computationally heavy when an accuracy in range cell migration correction is required

The Stolt interpolation algorithm is very accurate but computationally intensive due to heavy interpolation involved. It has advantages over the Range-Doppler algorithm.

7.0 CONCLUSION

This work focuses on the Range-Doppler technique and Stolt Interpolation technique in detail and their respective flow diagrams and important parameter expressions has been described in detailed. Also, the Range-Doppler technique and Stolt Interpolation technique were successfully implemented on Matlab to construct the SAR image and the two algorithms were compared.

8.0 REFERENCES

[1] Teng Long, Cheng Hu, Zegang Ding, Xichao Dong, Weiming Tian, Tao Zeng. "Geosynchronous SAR: System and Signal Processing", Springer Science and Business Media LLC, 2018

[2] Advances in Decision Sciences, Image Processing, Security and Computer Vision", Springer Science and Business Media LLC, 2020

[3] Didier Massonnet, Jean-Claude Souyris Imaging with synthetic aperture radar

[4] Frdric Adragna. "Synthetic Aperture Radar Images",Processing of Synthetic Aperture Radar Images, 01/01/2008

[5] Chen, Kunshan Principles of synthetic aperture radar signal processing

[6] Soumekh M. Synthetic Aperture Radar Signal Processing with Matlab algorithms

[7] Teng Long et al. Geosynchronous SAR System and Signal Processing Springer (2018)

[8] https://saredu.dlr.de/unit/SAR_imaging

[9] Bu-Chin Wang-Digital Signal Processing Technique

[10] Schlutz M.-Synthetic Aperture Radar Imaging Simulated in matlab

[11] John C. Curlander, Robert N. McDonough-Synthetic Radar Signal processing.

[12] Walter G. Carrara, Ron S. Goodman Ronald M Majewski-Spotlight Synthetic Aperture Radar Signal Processing Algorithms.

[13] Robert Wang, Yunkai Deng.-"Bistatic SAR System and Signal Processing Technology", Springer Science and Business Media LLC, 2018

[14] srmap.edu.in

[15] Spotlight Synthetic Aperture Radar", Principles of Modern Radar Advanced techniques, 2012.

[16] www.transint.boun.edu.tr

[17] Wu, Huaming.-"Motion Compensation for Near-Range Synthetic Aperture Radar Applications", KIT Scientific Publishing, Karlsruhe, 2012.

[18] Remote Sensing and Digital Image Processing, 2001

[19] Clay Stewart.-Synthetic Aperture Radar Algorithm

[20] Thuy Le Toan- Introduction to SAR Remote Sensing

[21] Mark A. Richards-Fundamentals of Radar Signal Processing